^{13}C NMR study on the charge-ordering salt α'-(BEDT-TTF)$_2$IBr$_2$

Shinji Hirose and Atsushi Kawamoto*

Department of Quantum and Condensed Matter Physics, Hokkaido University, Kita-ku, Sapporo, Hokkaido 060-0810, Japan

(Received 1 June 2009; revised manuscript received 3 September 2009; published 2 October 2009)

Among quasi-two-dimensional organic conductors, (BEDT-TTF)$_2X$, what form the two column structure of α or θ is thought to show a charge-ordering insulating state. The α' modification is the other candidate for a charge-ordering state. To determine the existence of a charge-ordering state and electron magnetism in the α' phase, which has a symmetry that differs from that of the α and θ phases, we utilized ^{13}C-NMR to examine α'-(BEDT-TTF)$_2$IBr$_2$ in which one side of the central carbon on the BEDT-TTF molecule is substituted with ^{13}C nuclei. We observed changes in its spectrum at 200 K. The angular dependence of the NMR shift at 15 K indicated that the charge-ordering pattern is intracolumn disproportionation and the ratio of charge disproportionation on the spin-poor site and spin-rich sites is almost 1:0. The angle dependence of NMR spectrum at 60 K suggests that the hyperfine coupling tensor in the paramagnetic charge-ordering state is determined not only by the charge density of on-site molecules but also by the contribution of off-site molecules. The change in hyperfine coupling tensor must be taken into account in NMR studies of the paramagnetic CO state.

DOI: 10.1103/PhysRevB.80.165103 PACS number(s): 71.30.+h, 74.70.Kn, 76.60.−k

I. INTRODUCTION

Quasi-two-dimensional organic conductors described by the formula (BEDT-TTF)$_2X$ have the two-dimensional electronic structures in which two BEDT-TTF(bis-ethylenedithio-tetrathiafulvalene) molecules donate one electron to the monovalent anion X. Among these salts, the α and θ modifications, each of which has a double column structure tilted toward each other,[1–4] have quarter-filled band structures, whereas the κ modification, which has strong dimeric structure,[5,6] has an approximately half-filled band structure.[7] It is important for quarter-filled systems to examine both the on-site Coulomb repulsion, U, and the off-site Coulomb repulsion, V, and these systems are likely to show charge-order (CO) state.[8] Indeed, a CO state was confirmed in α-(BEDT-TTF)$_2$I$_3$ and θ-(BEDT-TTF)$_2$RbZn(SCN)$_4$ and in similar salts.[9–14] Moreover, superconductivity was observed in α-(BEDT-TTF)$_2$I$_3$ under uniaxial stress and in θ-(BEDT-TTF)$_2$I$_3$ (Refs. 15 and 16) under ambient pressure. A relationship has been suggested between the superconductivity and the charge fluctuation.[17] The physics of CO has been recognized as an important topic in strongly correlated electron systems.[8]

The CO state shows various magnetic properties and depends on the crystal structure. For α-(BEDT-TTF)$_2$I$_3$, the space group is $P\bar{1}$ and this salt consists of three crystallographically independent molecules, A, B, and C. There are inversion centers between the two A molecules, with the B and C molecules present in the inversion center.[2] This salt shows a CO transition at 135 K, leading to the opening of a magnetic gap and the system assuming a spin singlet state.[18] In contrast, θ-(BEDT-TTF)$_2$RbZn(SCN)$_4$ has one crystallographically independent molecule in unit cell and the space group is $I222$.[1] This salt shows a CO transition at 190 K; however, due to crystal symmetry, the gap does not open and the system maintains its paramagnetism. At low temperature, spin-Peierls transition occurs and the system is in a spin singlet state.[19] Thus, the magnetism in the CO state strongly depends on crystal symmetry. To explore the CO state, a novel CO system, which has different crystal symmetry, is desired.

One candidate for a novel CO system is α'-(BEDT-TTF)$_2$IBr$_2$, which has a double column structure similar to that of α and θ but has a different symmetry from the α and θ phases.[20] Figure 1(a) illustrates the crystal structure of this salt. It has two pairs of crystallographically inequivalent molecules, A and A′ and B and B′, which are associated with the inversion center. This salt is built from alternating sheets of an anion layer and a conducting layer along the c^* axis. The electrical conductivity of this salt shows an anomaly at 200 K and semiconducting behavior from 300 to 100 K.[21] Magnetic susceptibility increases until 60 K and shows a sharp drop at low temperature.[21] As this material has a structure similar to that of the α and θ phases, which hardly form dimers, a CO state is expected.

Recently, this material was assessed by Raman-scattering and infrared spectroscopy.[22] However the charge disproportionation has been observed above 200 K and there is not any qualitative changes at around 200 K where the conductivity showed the anomaly. Moreover, it was also suggested that by applying pressures, the charge disproportionation of this salt vanished and the anomaly observed at ambient pressure changed to metal-insulator (MI) transition with hysteresis.[22] It is important to reveal the nature of the anomaly and to

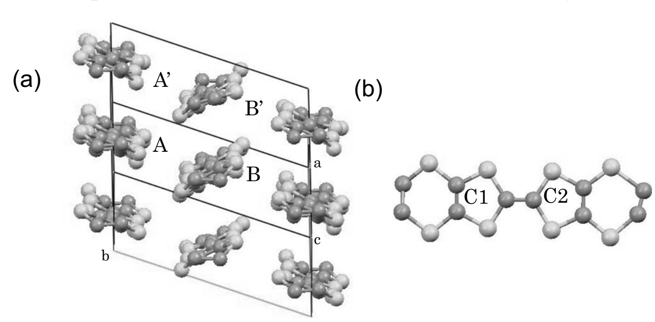

FIG. 1. (a) Crystal structure of α'-(BEDT-TTF)$_2$IBr$_2$ (Ref. 20). (b) Molecular structure of BEDT-TTF.

 ©2009 The American Physical Society

clarify whether the anomaly is a phase transition or not. If the anomaly is a phase transition, this salt gives valuable information about the connection between CO transition at ambient pressure and the conventional MI transition without the charge disproportionation under pressures and the different type of CO transition from those in α and θ modifications.

Vibrational spectroscopy detects the charge on molecules directly, whereas nuclear magnetic resonance (NMR) detects mainly magnetism in the salt. Addition to that, NMR observed the phenomenon with different time scale. Therefore NMR is complementary to vibrational spectroscopy and get the different information from the respect to the time scale. We have therefore utilized ^{13}C NMR to determine whether a CO state is present, as well as to assess the pattern of the CO state, and its magnetism.

II. EXPERIMENT

We utilized a single crystal of α'-(BEDT-TTF)$_2$IBr$_2$ in which one side of central carbon atoms in the BEDT-TTF molecules was substituted with ^{13}C nuclei using crosscoupling between thioketone and ketone. The coupling between thioketone and ketone reacts in preference to those between ketone and ketone, thioketone and thioketone. From mass spectroscopy, the crosscoupling molecule is major product (70%), the self-coupling molecule between ketones is second (26%) and the self-coupling molecule between thioketones is trace level (less than 4%).[23] Therefore the coupling with enriched thioketone and cooled ketone produces one side of central carbon enriched BEDT-TTF as major product and no enriched BEDT-TTF as minor product. By using this molecule, we could prevent the splitting caused by Pake doublets while easily performing quantitative experiments. The crystal was prepared electrochemically from BEDT-TTF molecules and (n-Bu)$_4$NIBr$_2$ in 1,1,2-trichrolo-ethane. We confirmed its α' structure and determined its crystal orientation by x-ray diffraction.

NMR measurements were performed with decreasing temperature under a field of 9.4 T and the spectra were obtained by fast Fourier transformation of the echo signal with a $\pi/2-\pi$ pulse sequence. Spin-lattice relaxation time was determined by the saturation recovery method.

III. RESULTS AND DISCUSSION

A. Peak assignment of NMR spectrum

Two central carbon atoms are present in the crystalline state of BEDT-TTF molecules, represented by C1 and C2 [Fig. 1(b)]. As there are two ^{13}C sites each on the A and B molecules, four NMR lines were expected from these sites. We applied a magnetic field parallel to the *ab* plane of this salt and obtained an NMR spectrum consisting of four peaks (Fig. 2). To properly assign peaks, we assessed the angular dependence of the NMR spectrum. Figure 3 shows the angular dependence of the NMR spectrum with a field parallel to the *ab* plane, with an angle of 0° corresponding to the *b* axis.

In the rotation of this plane, the NMR shift is almost decided by the angular dependence of the Knight shift. In a paramagnetic state, the Knight shift also depends on the direction of the magnetic field against the $2p_z$ orbital, which is perpendicular to the molecular plane of BEDT-TTF. The Knight shift is maximal when magnetic field is parallel to the $2p_z$ orbital and minimal when the magnetic field is applied perpendicular to the $2p_z$ orbital. Figure 4 illustrates the projection of the molecular sheet of α'-(BEDT-TTF)$_2$IBr$_2$ on the *ab* plane.[20] The NMR shift should be minimal at 177° for the B molecule and at 45° for the A molecule. Hence the two filled square plots in Fig. 3, with a minimum shift at 45° were identified as A, whereas the two filled circle plots in Fig. 3, with a minimum shift minimizes at 177° were identified as B.

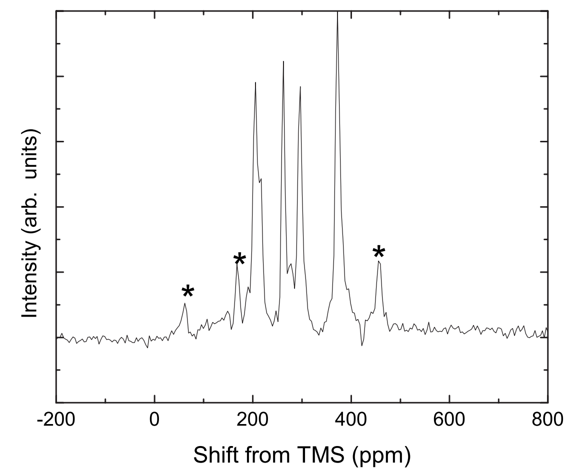

FIG. 2. NMR spectrum in textitab plane at 294 K (*: peak from small piece on a single crystal).

B. Temperature dependence of the NMR spectrum

After assigning the four peaks observed in room temperature, we measured the temperature dependence of NMR spectrum at the angle of the dotted line in Fig. 3. Figure 5 shows the temperature dependence of the NMR spectrum. Although four sharp peaks were observed at room temperature, the spectrum became broader near 210 K. Below 200 K,

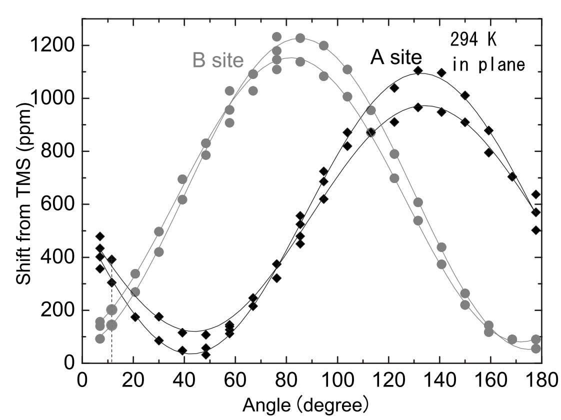

FIG. 3. Angular dependence of NMR spectrum at room temperature. The dotted line corresponds to the angle in Figs. 2, 5, and 7.

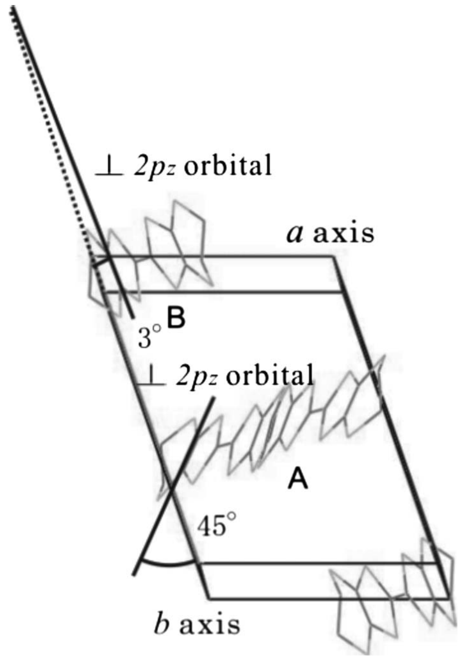

FIG. 4. Crystal structure of α'-(BEDT-TTF)$_2$IBr$_2$ along the c^* axis.

the spectrum consisted of four sharp peaks, which shifted with deceasing temperature and two broad peaks.

Whereas the phenomena of a slow exchange and static state are indistinguishable in Raman scattering, NMR spectrum discontinuously changes at around 200 K. When the rate of a slow exchange becomes merely slower, NMR spectrum should change continuously. Moreover NMR can probe such slow phenomenon as the line broadening from phenomenological width due to the static rigid lattice. The line width below 200 K is comparable to the phenomenological width, suggesting that the electronic state is static.

The four sharp peaks could be interpreted as signals from C1 and C2 of the spin-poor A and B sites, whereas the broad peaks could be interpreted as spin-rich sites. As spin susceptibility decreased, each peak shifted to lower frequency, enabling the broad peaks to be observed more clearly. These spectrum peaks at 15 K consisted of two pairs of doublet spectrum peaks, resembling the behavior of the CO state in θ-(BEDT-TTF)$_2$RbZn(SCN)$_4$.[9] Considering the NMR results for the latter salt, the peak we observed around 70 ppm at 15 K was likely to be the spin-rich site, whereas the peak observed around 180 ppm was likely to be spin-poor site. To confirm these assignments, we measured spin-lattice relaxation time, T_1, at 15 K. T_1 of the two peaks at higher frequency is 40 s, whereas T_1 of the two peaks at lower frequency is 40 ms. Qualitatively, T_1 at the spin-rich site is faster than that at the spin-poor site. We therefore concluded that the two low-frequency peaks were spin-rich sites, the two high-frequency peaks were spin-poor sites and the separation of spin susceptibility is almost 1:0. From the discontinuous changes in the spectrum at around 200 K and the peak assignment, we can come the draw that the anomaly at around 200 K is CO transition.

Raman-scattering spectroscopy suggested that the ratio of charge disproportionation between rich and poor sites was 9:1.[24] Hence we concluded that the transition at 200 K was a CO transition, as same as in θ-(BEDT-TTF)$_2$RbZn(SCN)$_4$.

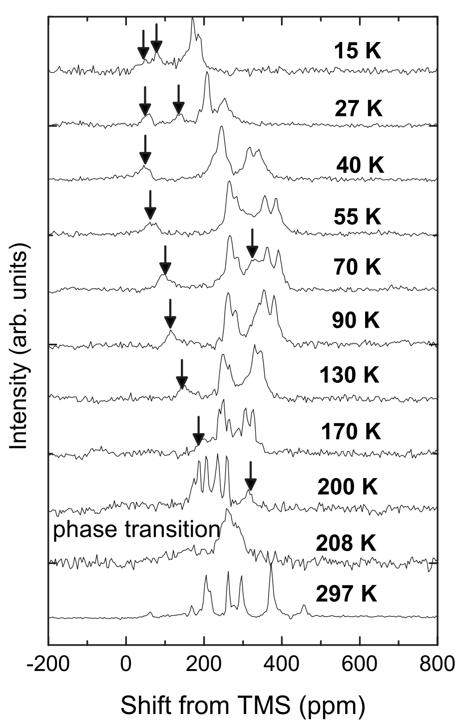

FIG. 5. Temperature dependence of the NMR spectrum at the angle of the dotted line in Fig. 3. (Down arrows represent peaks from rich sites.)

C. Charge pattern in the CO state

It is important to determine the pattern of charge disproportionation in the CO state. Using technique such as Raman spectroscopy, the degree of charge disproportionation can be observed but information about the pattern of charge disproportionation cannot. NMR, however, can obtain this information from the angular dependence of the NMR spectrum. The pattern of CO can be roughly classified as intracolumn or intercolumn disproportionation. If our conclusions in Sec. III B are right, the four peaks likely represent as A-rich, B-rich, A-poor, and B-poor sites. Moreover, the difference at the two carbon site between C1 and C2 will become little; i.e., the charge pattern will be intracolumn disproportionation, similar to the horizontal or diagonal pattern. In other cases, the four peaks can be assigned as the two carbon sites, C1 and C2, from the A(B)-poor site and the B(A)-rich site; i.e., the charge pattern will be intercolumn disproportionation, similar to the vertical pattern. We therefore measured the angular dependence of these peaks to verify the CO pattern and our peak assignment in paramagnetic CO state. Figure 6 shows the angular dependence of the NMR shift at 15 K. We observed two peaks (filled circles and filled squares) with large amplitude and other peaks (open circles and open squares) with small amplitude.

When we focused on the phase of the angular dependence, one of the large amplitude sites (filled circles) had a

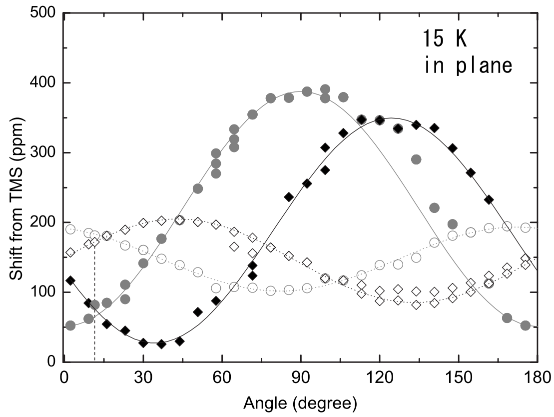

FIG. 6. Angular dependence of NMR shift in *ab* plane at 15 K. The dotted line corresponds to the angle in Figs. 2, 5, and 7.

phase opposite to one of the small amplitude sites (open circles), whereas the other large amplitude site (filled squares) had a phase opposite to that of another small amplitude site (opened squares). Compared with Fig. 3, one of rich sites with large amplitude (filled circles) had the same phase as molecule B and another rich site (filled squares) had the same phase as molecule A. Hence the filled circles represent the B-rich site, the open circles represent the B-poor site, the filled squares represent the A-rich site, and the open squares represent the A-poor site.

NMR shift, δ, can be expressed as the sum of the Knight Shift, K, and the chemical shift, σ. The phase of the chemical shift is opposite to that of the Knight shift.[14] As the temperature decreased from 60 K, the spin susceptibility of the salt decreased, almost vanishing at 15 K. Therefore at 15 K on the poor site, the NMR shift is due mainly to the chemical shift. This means that the degree of charge disproportionation is almost 1:0, consistent with the results of T_1 and Raman spectroscopy. These results strongly suggest that the pattern of CO is intracolumn disproportionation with large charge disproportionation.

D. Hyperfine coupling constant in the paramagnetic CO state

Figure 7 shows the temperature dependence of the NMR shift. The Knight shift is proportional to spin susceptibility. The hyperfine coupling constants of the two carbon site peaks in the A column were positive and almost zero, whereas those in the B column were negative and almost zero above the CO transition. The hyperfine coupling constant in the A or B column below the CO transition, however, seemed to be positive. In many previous studies, the discussion of CO state in NMR was based on the assumption that Knight shift is expressed as $a_0(1\pm\Delta\rho/2)\chi_s$,[9] where a_0 is the hyperfine coupling constant above the CO transition and $\Delta\rho$ is the degree of charge disproportionation. These assumptions were the basis of the quantitative NMR determination of the paramagnetic CO state. Results showing that the hyperfine coupling constants at all sites were positive in the CO state were inconsistent with the hyperfine coupling constants in the metallic state. To resolve this inconsistency, site assignment of the peaks in the paramagnetic CO state was

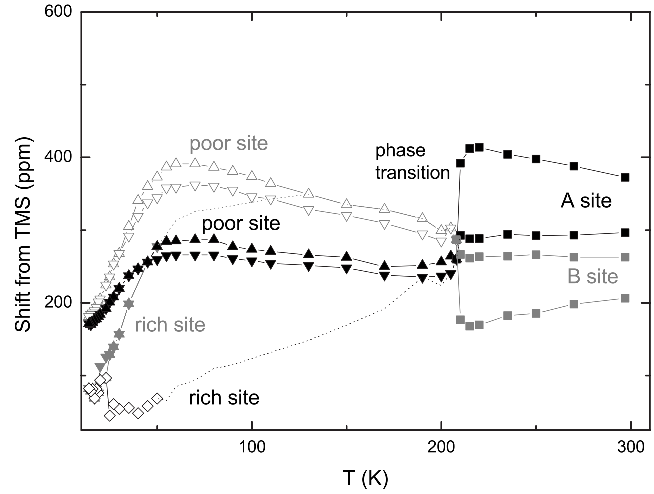

FIG. 7. Temperature dependence of the NMR shift at the angle of dotted line in Fig. 3.

performed. For site assignment of poor sites under paramagnetic CO phase, we rotated the salt in the *ab* plane at 60 K. Figure 8 shows the angular dependence of the NMR shift at 60 K. The two peaks represented by open symbols showed large amplitude with the same phase, whereas the two peaks represented by filled symbols showed small amplitude with same phase. Hence we could assign the two opened symbol as being from a single molecular site and the two filled symbols as being from another molecular site. Surprisingly, both shifts have different principle axes at both room temperature and 15 K, suggesting the changes in the hyperfine coupling tensor after the CO transition.

The Knight shift can be regarded as a sum of the contribution from on-site and off-site molecules. Above 200 K (Fig. 9, left), the local spin susceptibility at each site was same; therefore, the hyperfine coupling tensor can be expressed as $\mathbf{A}+\Sigma_i\mathbf{B}_i$ and the hyperfine coupling constant as $a_0=\tilde{\mathbf{h}}(\mathbf{A}+\Sigma_i\mathbf{B}_i)\mathbf{h}$. Here $\mathbf{h}$ is a direction cosine of the external field on molecular coordinates, and $\mathbf{A}$ and $\mathbf{B}_i$ are hyperfine coupling tensors from on-site and off-site molecules, respectively. In contrast, considering the charge disproportionation below the phase transition (Fig. 9, right), the Knight shift on

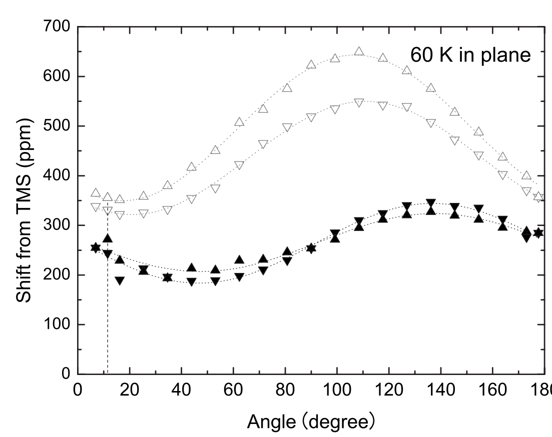

FIG. 8. Angular dependence of NMR shift in *ab* plane at 60 K. The dotted line corresponds to the angle in Figs. 2, 5, and 7.

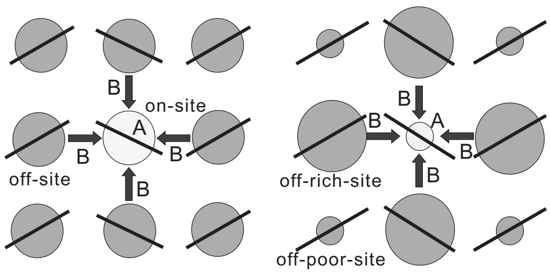

FIG. 9. Hyperfine coupling field around the molecular site. Left-fin non-CO state and right-fin diagonal CO state (poor on site).

the rich site, K_r, and the poor site, K_p, can be expressed as

$$K_p = \tilde{\mathbf{h}}\mathbf{A}\mathbf{h}\chi_p + \sum_i \tilde{\mathbf{h}}\mathbf{B}_i\mathbf{h}\chi_r, \quad (1)$$

$$K_r = \tilde{\mathbf{h}}\mathbf{A}\mathbf{h}\chi_r + \sum_i \tilde{\mathbf{h}}\mathbf{B}_i\mathbf{h}\chi_p, \quad (2)$$

respectively. Here χ_p and χ_r are the local spin susceptibility on the poor site and rich site, respectively. Since the degree of charge disproportionation was almost 1:0 at these sites, the Knight shift on the poor site, K_p, was almost equal to $\Sigma_i\tilde{\mathbf{h}}\mathbf{B}_i\mathbf{h}\chi_r$ and had a different angular dependence from that above 200 K.

These results call attention to the NMR application on paramagnetic CO state. In the NMR study of CO material, the analysis were based on the formulas, $K = a_0(1\pm\Delta\rho/2)\chi_s$ and $T_1^{-1} \propto a_0^2(1\pm\Delta\rho/2)^2$. However our results suggested that K and T_1 depended not only on local susceptibility, $(1\pm\Delta\rho/2)\chi_s$, but on the change in the hyperfine coupling tensor. Thus, for CO state, which showed large charge disproportionation, the ratio of charge ρ_r/ρ_p was not K_r/K_p and $(T_{1,p}/T_{1,r})^{1/2}$. Here, K_r and K_p are Knight shift at the rich and poor sites, respectively, and $T_{1,r}$ and $T_{1,p}$ were T_1 on rich site and poor site, respectively.

The angular dependence at 15 K suggested charge disproportionation on the intracolumns. Simple intracolumn model is horizontal or diagonal. But, in the case of these patterns, the amplitude at the A and B sites were each expected to be almost the same in the paramagnetic CO state. However, we observed a difference in amplitude at the two site (Fig. 8). These results suggest that the charge disproportionation pattern is not a simple horizontal or diagonal structure but is more complicated.

E. Relation between CO transition and spin gap generation

The electrical conductivity of α-(BEDT-TTF)$_2$I$_3$ and θ-(BEDT-TTF)$_2$RbZn(SCN)$_4$ showed clear metal-insulator transition due to CO transition. In contrast, α'-(BEDT-TTF)$_2$IBr$_2$ showed semiconductive behavior above and below 200 K with only activation energy showing a change at this temperature.[1,2]

Although Raman spectroscopy suggested that CO was already present above 200 K,[24] NMR showed a clear CO transition at 200 K. The difference between two measurements is due to their respective time scale. Raman spectroscopy can resolve fast phenomenon, whereas NMR can resolve slower phenomenon, less than ~ MHz. Therefore the fluctuation in CO likely develops above 200 K and the static CO transition emerges at 200 K. This fluctuation may contribute to the semiconductive behavior of this material above 200 K. In θ-(BEDT-TTF)$_2$RbZn(SCN)$_4$, the translation symmetry was maintained, and a gap was not present at the temperature of CO transition, and the spin-Peierls transition occurs at lower temperature. In α-(BEDT-TTF)$_2$I$_3$ salt, however, CO transition occurs with the system in a dimeric structure and goes into the spin-Peierls state.[1,18] The relationship between magnetism and symmetry in the CO state of this salt is interesting. Crystal symmetry of this salt suggests that, when CO occurs, the electronic system should go into the spin-Peierls state, similar to α-(BEDT-TTF)$_2$I$_3$ salt. However spin susceptibility showed paramagnetic behavior, such as θ-(BEDT-TTF)$_2$RbZn(SCN)$_4$ salt, suggesting that its gap energy was less than that of α-(BEDT-TTF)$_2$I$_3$. The complicated intracolumn charge pattern may decrease the gap energy.

IV. CONCLUSION

^{13}C-NMR of α'-(BEDT-TTF)$_2$IBr$_2$ showed a clear change in spectrum shape at 200 K, indicative of CO transition. From its angular dependence and nuclear relaxation time, T_1, at 15 K, this salt likely forms an intracolumn charge pattern, with a degree of charge disproportionation of almost 1:0 and the charge disproportionation pattern is not a simple horizontal or diagonal structure but is more complicated. The angular dependence at 60 K suggests that the hyperfine coupling tensor is expressed not only by on-site contribution but also by off-site contribution. Therefore, the change in hyperfine coupling tensor must be taken into account in NMR studies of the paramagnetic CO state.

ACKNOWLEDGMENTS

The authors wish to thank K. Kumagai, Y. Furukawa (Hokkaido Univ.) for stimulating discussions, and K. Yakushi and K. Yamamoto (Institute for Molecular Science) for the discussions of Raman and IR studies. The authors also wish to thank T. Kawai for his experimental supports. This study was supported in part by a Grant-in-Aid for Scientific Research (Grant No. 18540306) from the Ministry of Education, Culture, Sports, Science, and Technology of Japan.

*atkawa@phys.sci.hokudai.ac.jp

[1] H. Mori, S. Tanaka, and T. Mori, Phys. Rev. B **57**, 12023 (1998).
[2] K. Bender, I. Hennig, D. Schweitzer, K. Dietz, H. Endres, and H. J. Keller, Mol. Cryst. Liq. Cryst. **108**, 359 (1984).
[3] H. Kobayashi, R. Kato, A. Kobayashi, Y. Nishino, K. Kajita, and W. Sasaki, Chem. Lett. **15**, 833 (1986).
[4] R. Kato, H. Kobayashi, A. Kobayashi, Y. Nishino, K. Kajita, and W. Sasaki, Chem. Lett. **15**, 957 (1986).
[5] H. Urayama, H. Yamochi, G. Saito, S. Sato, A. Kawamoto, J. Tanaka, T. Mori, Y. Maruyama, and H. Inokuchi, Chem. Lett. **17**, 463 (1988).
[6] H. Urayama, H. Yamochi, G. Saito, K. Nozawa, T. Sugano, M. Kinoshita, S. Sato, K. Oshima, A. Kawamoto, and J. Tanaka, Chem. Lett. **17**, 55 (1988).
[7] K. Kanoda, Physica C **282-287**, 299 (1997).
[8] H. Seo and H. Fukuyama, J. Phys. Soc. Jpn. **66**, 1249 (1997).
[9] K. Miyagawa, A. Kawamoto, and K. Kanoda, Phys. Rev. B **62**, R7679 (2000).
[10] K. Yamamoto, S. Iwai, S. Boyko, A. Kashiawazaki, F. Hiramatsu, C. Okabe, N. Nishi, and K. Yakushi, J. Phys. Soc. Jpn. **77**, 074709 (2008).
[11] R. Wojciechowski, K. Yamamoto, K. Yakushi, M. Inokuchi, and A. Kawamoto, Phys. Rev. B **67**, 224105 (2003).
[12] T. Kakiuchi, Y. Wakabayashi, H. Sawa, T. Takahashi, and T. Nakamura, J. Phys. Soc. Jpn. **76**, 113702 (2007).
[13] K. Yamamoto, K. Yakushi, K. Miyagawa, K. Kanoda, and A. Kawamoto, Phys. Rev. B **65**, 085110 (2002).
[14] T. Kawai and A. Kawamoto, J. Phys. Soc. Jpn. **78**, 074711 (2009).
[15] B. Salameh, A. Nothardt, E. Balthes, W. Schmidt, D. Schweitzer, J. Strempfer, B. Hinrichsen, M. Jansen, and D. K. Maude, Phys. Rev. B **75**, 054509 (2007).
[16] N. Tajima, A. E. Tajima, M. Tamura, Y. Nishio, and K. Kajita, J. Phys. Soc. Jpn. **71**, 1832 (2002).
[17] J. Merino and R. H. McKenzie, Phys. Rev. Lett. **87**, 237002 (2001).
[18] B. Rothaemel, L. Forró, J. R. Cooper, J. S. Schilling, M. Weger, P. Bele, H. Brunner, D. Schweitzer, and H. J. Keller, Phys. Rev. B **34**, 704 (1986).
[19] T. Nakamura, W. Minagawa, R. Kinami, Y. Konishi, and T. Takahashi, Synth. Met. **103**, 1898 (1999).
[20] M. Watanabe, M. Nishikawa, Y. Nogami, and K. Oshima, J. Korean Phys. Soc. **31**, 95 (1997).
[21] M. Tokumoto, H. Anzai, T. Ishiguro, G. Saito, H. Kobayashi, R. Kato, and A. Kobayashi, Synth. Met. **19**, 215 (1987).
[22] Y. Yue, C. Nakano, K. Yamamoto, M. Uruichi, R. Wojciechowski, M. Inokuchi, K. Yakushi, and A. Kawamoto, J. Phys. Soc. Jpn. **78**, 044701 (2009).
[23] M. Yamashita, A. Kawamoto, and K. Kumagai, Synth. Met. **133-134**, 125 (2003).
[24] Y. Yue, C. Nakano, K. Yamamoto, M. Uruichi, K. Yakushi, and A. Kawamoto, J. Phys.: Conf. Ser. **132**, 012007 (2008).